The Journal of Neuroscience, August 1990, 10(8): 2513–2527

Immunocytochemical Localization of the Neuron-Specific Form of the c-*src* Gene Product, pp60$^{c\text{-}src(+)}$, in Rat Brain

Mary M. Sugrue,[1] Joan S. Brugge,[1,2] Daniel R. Marshak,[3] Paul Greengard,[4] and Eric L. Gustafson[4]

[1]Department of Microbiology, SUNY at Stony Brook, Stony Brook, New York 11794, [2]Howard Hughes Medical Institute and Department of Microbiology, University of Pennsylvania School of Medicine, Philadelphia, Pennsylvania 19104, [3]Cold Spring Harbor Laboratory, Cold Spring Harbor, New York, 11724, and [4]Laboratory of Molecular and Cellular Neuroscience, The Rockefeller University, New York, New York 10021

Neurons express high levels of a variant form of the c-*src* gene product, denoted pp60$^{c\text{-}src(+)}$, which contains a 6 amino acid insert in the amino-terminal half of the c-*src* protein. We have determined the localization of pp60$^{c\text{-}src(+)}$ in neurons using an affinity-purified anti-peptide antibody, referred to as affi-SB12, that exclusively recognizes this neuron-specific form of the c-*src* gene product. Using affi-SB12, we examined the distribution of pp60$^{c\text{-}src(+)}$ by immunoperoxidase staining of sections through adult rat brains. pp60$^{c\text{-}src(+)}$ was widely distributed in rat brain and appeared to be differentially expressed in subpopulations of neurons. The majority of immunoreactive neurons was found in the mesencephalon, cerebellum, pons, and medulla. Telencephalic structures that contained substantial populations of pp60$^{c\text{-}src(+)}$-immunoreactive neurons included layer V of the cerebral cortex and the ventral pallidum. Within individual neurons, pp60$^{c\text{-}src(+)}$ immunoreactivity was localized to the cell soma and dendritic processes, while labeling of axons and nerve terminals (puncta) was not as readily detected. Dense accumulations of immunoreactive axons were rare, being most prominent in portions of the inferior and superior olive, and in the spinal trigeminal nucleus. While the regional distribution of pp60$^{c\text{-}src(+)}$ immunoreactivity does not correlate with any specific neuronal cell type or first messenger system, this unique pattern of expression of pp60$^{c\text{-}src(+)}$ suggests the existence of a previously uncharacterized functional organization within the brain. Furthermore, the localization of this neuron-specific tyrosine kinase in functionally important areas of the nerve cell, namely, dendritic processes, axons, and nerve terminals, suggests that pp60$^{c\text{-}src(+)}$ may regulate pleiotropic functions in specific classes of neurons in the adult central nervous system.

The proto-oncogene c-*src* is homologous to the retroviral transforming gene v-*src* of Rous sarcoma virus (for reviews, see Bishop, 1983; Golden and Brugge, 1988; Cooper, 1989). This cellular gene is highly conserved throughout evolution and has been found in such widely divergent species as human (Levy et al., 1984; Anderson et al., 1985; Sorge et al., 1985; Bolen et al., 1987), chicken (Stehelin et al., 1976; Takeya and Hanafusa, 1983), fish (Barnekow et al., 1982), fruit fly (Shilo and Weinberg, 1981; Hoffman-Falk et al., 1983; Simon et al., 1983; Gregory et al., 1987), and sponge (Barnekow and Schartl, 1984). The c-*src* gene encodes a 60 kDa phosphoprotein, pp60$^{c\text{-}src}$, which functions as a tyrosine-specific protein kinase (for reviews, see Hunter and Cooper, 1985; Golden and Brugge, 1988; Cooper, 1989). To date the physiological role of pp60$^{c\text{-}src}$ has not been identified. However, several lines of evidence suggest that the c-*src* gene product may serve a specialized function in neurons. High levels of pp60$^{c\text{-}src}$ have been detected in brain and in other neural tissues of vertebrates (Cotton and Brugge, 1983; Gessler and Barnekow, 1984; Levy et al., 1984; Bolen et al., 1985; Fults et al., 1985; Shores et al., 1987; Cartwright et al., 1988) and in *Drosophila* (Simon et al., 1985). The expression of c-*src* in neural tissues appears to be developmentally regulated as pp60$^{c\text{-}src}$ is initially expressed at the onset of neuronal differentiation and then is maintained at high levels in postmitotic, fully differentiated neurons in the adult central nervous system (Schartl and Barnekow, 1984; Sorge et al., 1984; Fults et al., 1985; Simon et al., 1985; Lynch et al., 1986; Maness, 1986; Maness et al., 1986; Vardimon et al., 1986; Cartwright et al., 1987, 1988; Gregory et al., 1987; LeBeau et al., 1987; Mellström et al., 1987; Wiestler and Walter, 1988). A unique form of the c-*src* gene product has since been identified in neurons (Brugge et al., 1985). This protein, designated pp60$^{c\text{-}src(+)}$, is expressed at high levels in neurons and is structurally and enzymatically distinct from the pp60$^{c\text{-}src}$ molecule expressed in non-neuronal cells (Brugge et al., 1985, 1987a). This neuron-specific form of the c-*src* gene product, which contains a 6 amino acid insert in the amino-terminal half of the c-*src* protein, is encoded by a unique c-*src* mRNA. This alternately spliced c-*src* transcript found in neurons contains an 18 base-pair insertion which was mapped directly to the intron between exons 3 and 4 of the c-*src* gene (Levy et al., 1987; Martinez et al., 1987; Raulf et al., 1989a). This 18 base-pair mini-exon has been detected in chick (Levy et al., 1987), mouse (Martinez et al., 1987), human (Pyper and Bolen, 1989), and fish (Raulf et al., 1989a, b), but is absent in *Hydra* (Raulf et al., 1989a). The 6 amino acids encoded by the neuron-specific insert are completely conserved in chicken (Levy et al., 1987), mouse (Martinez et al., 1987), and human (Pyper

Received Dec. 28, 1989; revised Mar. 19, 1990; accepted Mar. 21, 1990.

This work was supported by grants CA-28146 and CA-47572 from the NIH to J.S.B. and M.M.S., USPHS Program Project Grant MH-40899 to P.G. and E.L.G., and NSF grant #BNS8707558 to D.R.M. We thank Joan Levy for providing the CEF/c-*src* and CEF/c-*src*(+) cells, and Bill Studier for providing the T7 expression vector. We also thank Mike DeMarco and Donna Fossaceca for technical assistance; Paul Fisher, John Schmidt, and Helen Barbas for helpful discussions; Ivar Walaas for critical reading of this manuscript; Paula Enrietto for use of the immunofluorescence microscope; and Barry Swimar for photographic assistance.

Correspondence should be addressed to Dr. Joan S. Brugge, Howard Hughes Medical Institute, University of Pennsylvania School of Medicine, Clinical Research Building, Room 405, 422 Curie Boulevard, Philadelphia, PA 19104-6148.

and Bolen, 1989), whereas only 50% of these amino acids are conserved in fish (Raulf et al., 1989a). The specific activity of this variant form of c-*src* protein is elevated compared to that of pp60$^{c\text{-}src}$, as measured by tyrosine phosphorylation of the *src* substrate, p36, *in vivo* and by anti-phosphotyrosine immunoblots (Brugge et al., 1985; Cartwright et al., 1987; Levy and Brugge, 1989).

Several lines of evidence indicate that pp60$^{c\text{-}src(+)}$ is expressed specifically by neuronal cells. pp60$^{c\text{-}src(+)}$ is the major form of c-*src* protein expressed in primary neuron cultures, and it is not detected in cultured astrocytes or fibroblasts or in any non-neural tissues (Cotton and Brugge, 1983; Brugge et al., 1985; Pyper and Bolen, 1989). In addition, embryonal carcinoma cells that have been induced to differentiate into neuron-like cells by the addition of retinoic acid express high levels of pp60$^{c\text{-}src(+)}$ (Lynch et al., 1986). Similarly, this variant form of the c-*src* protein is expressed by primary neurons from rat embryo striatum that differentiate in culture (Cartwright et al., 1987). Several different human neuroblastoma cell lines express pp60$^{c\text{-}src(+)}$, whereas this unique form of the c-*src* gene product has not been detected in any glioblastoma cell lines (Bolen et al., 1985; Mellström et al., 1987; Yang and Walter, 1988). In addition to these *in vitro* analyses, there is evidence from *in vivo* studies that pp60$^{c\text{-}src(+)}$ is neuron-specific. Biochemical studies using mutant mice that display progressive degeneration of specific types of neurons indicate that there is a direct correlation between loss of neurons and a decrease in the levels of pp60$^{c\text{-}src(+)}$ (Brugge et al., 1987b). Moreover, neurochemical lesions of the rat caudate-putamen result in substantial losses of pp60$^{c\text{-}src(+)}$ in both the striatum and the substantia nigra, which is a major target nucleus for striatal efferents (Walaas et al., 1988). Together, these results provide further evidence that pp60$^{c\text{-}src(+)}$ is expressed by neurons *in vivo*.

The expression of a neuron-specific form of the c-*src* gene product suggests that pp60$^{c\text{-}src(+)}$ may play an important role in neuronal cell function. In an attempt to obtain further information on the functional significance of this tyrosine kinase in neurons, we have localized pp60$^{c\text{-}src(+)}$ in rat brain using an affinity-purified polyclonal anti-peptide antibody that exclusively recognizes only the variant form of the c-*src* protein without cross-reacting with pp60$^{c\text{-}src}$.

Materials and Methods

Antibodies. The peptide Asn-Asn-Thr-Arg-Lys-Val-Asp-Val-Arg-Glu-Gly-Asp, which contains the 6 amino acid insert of pp60$^{c\text{-}src(+)}$ (underlined), was designed as an antigen to produce a specific antibody to the insert region. Synthesis was performed by condensation of symmetric anhydrides of N-α-t-Boc-protected amino acids (Barany and Merrifield, 1979) on an Applied Biosystems 430A instrument using dimethyl formamide as the coupling solvent. Double coupling cycles were used for Asn and Arg, which were coupled as activated esters using 1-hydroxybenzotriazole. The side chains were protected as Tosyl-Arg, Asp-β-*O*-Benzyl, Thr-*O*-Benzyl, Glu-τ-*O*-Benzyl, and Lys-*N*-ϵ-chloro-benzyloxycarbonyl (all obtained from Applied Biosystems). The peptide was synthesized on a *p*-methyl-benzhydrylamine-derivatized, divinylbenzene-cross-linked, polystyrene resin, and the peptide cleaved from the support with liquid HF containing 5% (vol/vol) each of anisole and methylsulfide (Aldrich). The crude peptide was precipitated with diethyl ether, lyophilized, and redissolved in 10% (vol/vol) acetic acid. The peptide was desalted by gel filtration on a column (5 × 100 cm) of BioGel P-2 (BioRad) acrylamide resin and lyophilized. Final purification of the peptide was done by reverse phase HPLC on an octadecylsilanyl silica column (Waters). Amino acid analysis and sequence analysis by automated Edman degradation was used to verify the structure of the final product. The peptide was conjugated to Keyhole limpet hemocyanin in the presence of glutaraldehyde (Kagan and Glick, 1979). The conjugate was then used to immunize rabbits. The antisera obtained from these rabbits were screened for immunoreactivity with pp60$^{c\text{-}src}$ and pp60$^{c\text{-}src(+)}$ in immunoblot and immunoprecipitation assays. One pp60$^{c\text{-}src(+)}$-specific antiserum, referred to as SB12, was affinity-purified and then used in all localization studies of pp60$^{c\text{-}src(+)}$ described in this report. Monoclonal antibody 327 was prepared from mice immunized with pp60$^{v\text{-}src}$ expressed in *Escherichia coli* (Lipsich et al., 1983).

Affinity purification of pp60$^{c\text{-}src(+)}$-specific antibodies. The pp60$^{c\text{-}src(+)}$-specific antibodies were affinity-purified from the SB12 antiserum using a pp60$^{c\text{-}src(+)}$ affinity column. The c-*src*(+) protein that was used as ligand in preparing the affinity column was expressed in bacteria. The c-*src*(+) cDNA clone (Levy and Brugge, 1989) was inserted into an expression plasmid containing the T7 promoter (Rosenberg et al., 1987; M. Sugrue and J. Brugge, unpublished results). This construct was then used to transform the DE3 strain of *E. coli* that carries an integrated copy of the T7 polymerase gene (Rosenberg et al., 1987). pp60$^{c\text{-}src(+)}$ was isolated from these cells and coupled to CNBr-activated Sepharose 4B beads (Pharmacia, Piscataway, NJ). After application of antiserum to the column, the column was washed with 50 mM glycine, pH 2.3, and bound antibody was eluted with 50% ethylene glycol, pH 10.5.

Cells. Chicken embryo fibroblasts (CEFs) were infected with avian retrovirus vectors (Hughes et al., 1987) that encode a complete RSV genome with either c-*src* or c-*src*(+) replacing the viral *src* gene (Levy and Brugge, 1989). Cells were stained after 3 passages, when greater than 90% of the cells expressed pp60$^{c\text{-}src}$ or pp60$^{c\text{-}src(+)}$.

Immunoprecipitation. CEFs were labeled for 4 hr with 1 mCi/ml ^{32}P-orthophosphate in phosphate-free Dulbecco's modified medium. The cells were lysed in RIPA buffer (1% sodium deoxycholate, 1% Triton X-100, 158 mM NaCl, 5 mM EDTA, 10 mM Tris hydrochloride [pH 7.2], 0.1% SDS). Following clarification, the protein concentration was determined using the method of Lowry et al. (1951) and the lysates were adjusted to equal protein concentration. The clarified lysates were incubated with antibody and the immunoprecipitates were adsorbed to formalin-fixed *Staphylococcus aureus* (Pansorbin; Calbiochem-Behring San Diego, CA) as described previously (Levy and Brugge, 1989). The samples were subjected to electrophoresis on 7.5% SDS-polyacrylamide gels (Laemmli, 1970). The dried gels were exposed to X-Omat (Kodak) film using Lightning Plus (Dupont) intensifying screens at −70°C.

Indirect immunofluorescent cell staining. CEFs expressing high levels of either pp60$^{c\text{-}src}$ or pp60$^{c\text{-}src(+)}$ were seeded onto acid-etched 12 mm glass coverslips at 37°C. All subsequent steps were carried out at room temperature (RT). The cells were fixed using freshly prepared 2% formaldehyde in PBS for 20 min and then washed with 0.1 M glycine in PBS for 5 min. The coverslips were washed with PBS containing 0.1% BSA, 0.02% NaN_3, and 0.2% Triton X-100 (PBSAT) for 15 min. Fixed coverslips were either stored in PBSAT at 4°C or used immediately. Prior to the application of primary antibody, the cells were permeabilized with PBS containing 1% NP40, 0.1% BSA for 10 min, and then blocked with PBS containing 5% BSA for 30 min. A 1:100 dilution of affi-SB12 was applied to each coverslip and incubated for 1 hr. Then the coverslips were washed in PBSAT for 30 min. Biotinylated anti-rabbit IgG F(ab)$_2$ (Amersham) was diluted 1:100 using PBSAT and was applied to each coverslip for 1 hr. After washing with PBSAT for 30 min, FITC Streptavidin (Vector Laboratories, Burlingame, CA) was diluted 1:200 and then added for 1 hr. Finally, the coverslips were washed with PBS and then mounted onto microscope slides. Cells were observed using a Nikon microscope equipped with epifluorescent illumination.

Immunoperoxidase staining of fixed tissue sections. Male Sprague-Dawley rats (150–250 gm) were anesthetized with chloral hydrate (400 mg/kg, i.p.) and perfused transcardially with 200 ml of saline followed by 500 ml of freshly prepared 4% paraformaldehyde in 0.1 M phosphate buffer, pH 7.5. Brains were removed, post-fixed for 1 hr at 4°C, and then allowed to sink in 20% phosphate-buffered sucrose overnight at 4°C. Next, 50 μm-thick coronal or sagittal sections were cut using a vibratome. The sections were rinsed in 10 mM PBS, pH 7.5, and then blocked in 10% normal goat serum (Vector) for 10 min. Sections were then incubated with a 1:5 dilution of affinity-purified SB12 antibody, affi-SB12, overnight at RT. A modification of the avidin-biotin technique of Hsu et al. (1981) was used to localize pp60$^{c\text{-}src(+)}$ immunoreactivity. After being washed in PBS, the sections were first incubated with a 1:200 dilution of biotinylated goat anti-rabbit IgG (Vector) for 2 hr at RT and then with the ABC complex (Vector) for 2 hr at RT. The peroxidase reaction product was visualized using 0.04% (wt/vol), 3,3-diaminobenzidine (DAB, Sigma) and 0.012% (vol/vol) H_2O_2 in 0.1 M

phosphate buffer, pH 7.4. Sections were mounted on gelatin-coated slides and allowed to air-dry overnight at RT. Then the sections were dehydrated in an ascending series of alcohols, cleared in xylene, and a coverslip was applied using Permount (Fisher). A series of sections adjacent to those processed for immunocytochemistry was stained with cresyl violet for use in the identification of nuclear boundaries.

Light microscopy. The schematic diagrams shown in Figure 3 were drawn from the cresyl violet-stained sections described above, and the pp60$^{c\text{-}src(+)}$-immunoreactive neurons from the adjacent immunocytochemically processed sections were then plotted onto the drawings using a camera lucida attached to a Leitz microscope. Each dot on these diagrams represents approximately 5 cells. The distribution was taken from a single case and is representative of all the animals used in the study.

Results

Characterization of SB12, the pp60$^{c\text{-}src(+)}$-specific antiserum

The specificity of the SB12 antiserum was tested in immunoprecipitation assays using ^{32}P-labeled CEFs that were infected with retroviral vectors that allow high level expression of pp60$^{c\text{-}src(+)}$ (CEF/c-*src*(+)) or pp60$^{c\text{-}src}$ (CEF/c-*src*). Figure 1 demonstrates that the SB12 antiserum specifically recognized pp60$^{c\text{-}src(+)}$ and did not cross-react with pp60$^{c\text{-}src}$. SB12 immunoprecipitated pp60$^{c\text{-}src(+)}$ from the CEF/c-*src*(+) cells (*lane 7*); however, this antiserum did not recognize pp60$^{c\text{-}src}$ from the CEF/c-*src* cells (*lane 3*). In contrast, monoclonal 327, which recognizes both the c-*src* and c-*src*(+) gene products, immunoprecipitated pp60$^{c\text{-}src}$ (*lane 1*) and pp60$^{c\text{-}src(+)}$ (*lane 5*). Preadsorption of SB12 with the c-*src*(+) peptide antigen blocked immunoprecipitation of pp60$^{c\text{-}src(+)}$ (*lane 8*). Preimmune rabbit serum did not immunoprecipitate any specific protein(s) (*lanes 2, 6*). When SB12 antiserum was used to probe lysates prepared from rat brain in an immunoblot assay, a single protein that comigrated with a pp60$^{c\text{-}src(+)}$ marker was detected (data not shown).

Immunolocalization of pp60$^{c\text{-}src(+)}$ in chick embryo fibroblasts

In order to prepare the SB12 antiserum for use in immunolocalization studies, we affinity-purified the pp60$^{c\text{-}src(+)}$-specific antibodies using an affinity column containing bound pp60$^{c\text{-}src(+)}$ and used affi-SB12 in immunofluorescent cell staining of CEF overexpressor cells, CEF/c-*src*(+) and CEF/c-*src*. A positive signal of immunofluorescence was observed in the CEF/c-*src*(+) cells alone. A distinct pattern of immunofluorescence was observed in these fibroblasts expressing high levels of pp60$^{c\text{-}src(+)}$. As shown in Figure 2, staining was observed throughout the cytoplasm with enhanced staining in the perinuclear region of the cell. No immunofluorescence was detected when CEF/c-*src* cells were incubated with affi-SB12 (data not shown). A similar absence of immunofluorescence was observed when affi-SB12 was preincubated with the c-*src*(+) peptide antigen (data not shown). These results indicate that affi-SB12 is specific for pp60$^{c\text{-}src(+)}$ and does not cross-react with pp60$^{c\text{-}src}$.

Distribution of pp60$^{c\text{-}src(+)}$ immunoreactivity in rat brain

In most areas where perikarya could be visualized, pp60$^{c\text{-}src(+)}$ immunoreactivity was localized both in the cell body and in the dendritic processes of neurons. In contrast, staining of axons and axon terminals was not as readily detected, being most prominent in brain-stem structures. In the description of the distribution of pp60$^{c\text{-}src(+)}$ immunoreactivity below, presumed axons or axon terminals are referred to as puncta or varicosities. Staining was blocked by preincubation of affi-SB12 with the c-*src*(+) peptide antigen.

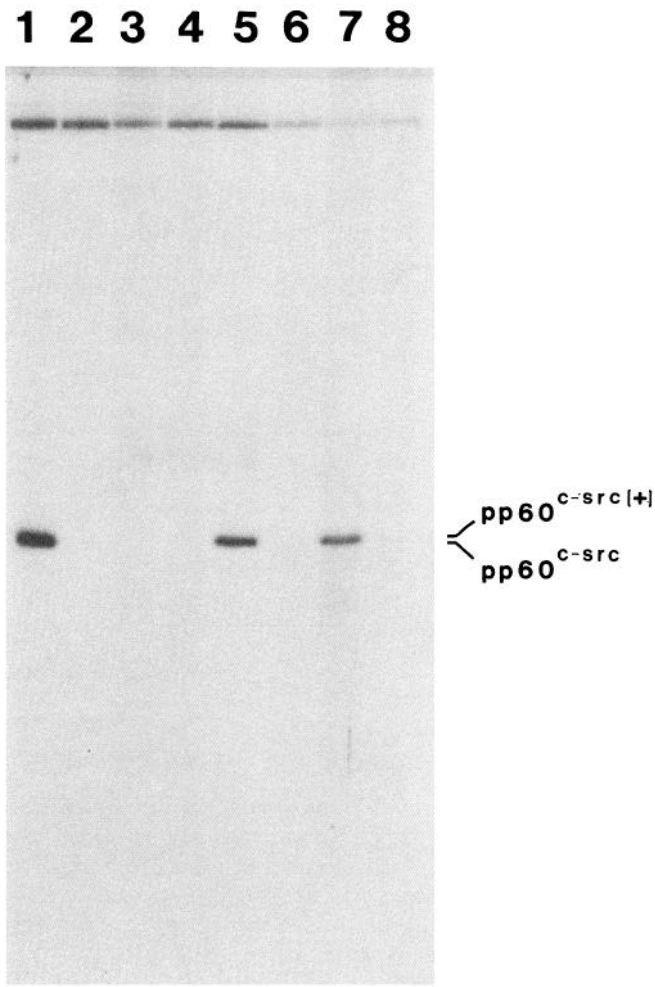

Figure 1. Characterization of SB12, the pp60$^{c\text{-}src(+)}$-specific antiserum. CEF cultures infected with RSVc-*src* virus (CEF/c-*src*, *lanes 1–4*) or RSVc-*src*(+) virus (CEF/c-*src*(+), *lanes 5–8*) were metabolically labeled with ^{32}P-orthophosphate. The *src* proteins were immunoprecipitated from CEF/c-*src* and CEF/c-*src*(+) cell lysates, respectively, with monoclonal antibody 327 (*lanes 1, 5*), preimmune rabbit serum (*lanes 2, 6*), SB12 antiserum (*lanes 3, 7*), and SB12 antiserum that was preadsorbed by the c-*src*(+) peptide antigen (*lanes 4, 8*). Immunoprecipitated *src* proteins were analyzed on a 7.5% SDS-polyacrylamide gel.

pp60$^{c\text{-}src(+)}$ immunoreactivity was widely distributed in the rat brain. Schematic diagrams of half coronal sections through the rat brain demonstrating the distribution of pp60$^{c\text{-}src(+)}$-containing neurons are shown in Figure 3, while axonal profiles are shown in subsequent figures. pp60$^{c\text{-}src(+)}$ was not detected in all neurons. Intensely immunoreactive neurons were visible in some areas, whereas moderately immunoreactive neurons were present in other brain regions. The following is a description of the distribution of pp60$^{c\text{-}src(+)}$ immunoreactivity through the rostral-caudal extent of the rat brain.

Pons/medulla

The pattern of pp60$^{c\text{-}src(+)}$ immunoreactivity in the inferior olive represents one of the best examples of axonal pp60$^{c\text{-}src(+)}$ immunoreactivity in the brain. Dense immunoreactive puncta were observed throughout the inferior olivary complex (Fig. 4). Scattered neuronal cell bodies were also stained. However, due to

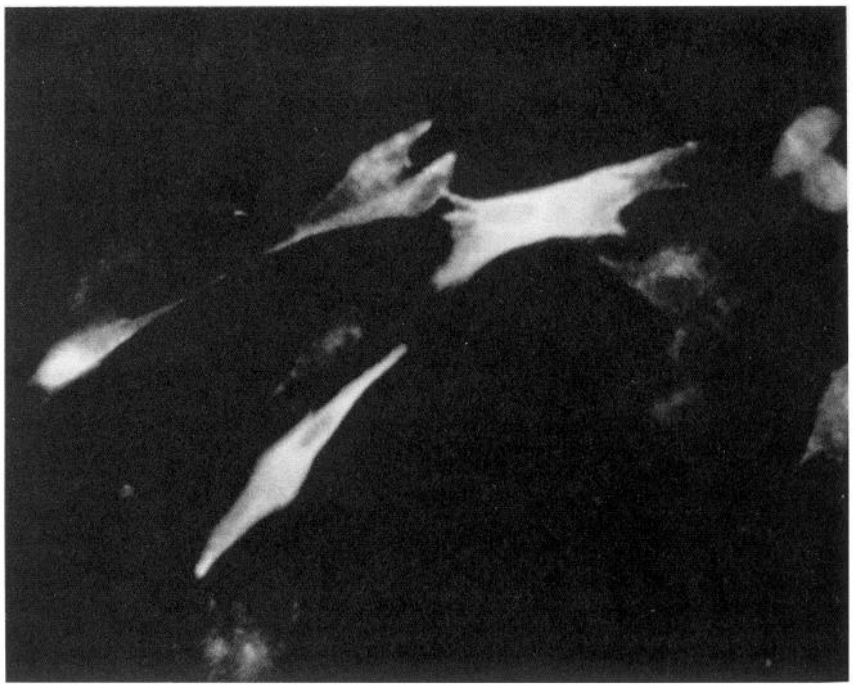

Figure 2. Immunofluorescent cell staining of chick embryo fibroblasts expressing pp60$^{c\text{-}src(+)}$. CEFs that were genetically engineered to express high levels of pp60$^{c\text{-}src}$ or pp60$^{c\text{-}src(+)}$ were stained using affi-SB12, biotinylated anti-rabbit IgG F(ab)$_2$, and FITC Streptavidin. Only CEF/c-*src*(+) cells exhibited intense immunofluorescent labeling using affi-SB12.

the dense immunoreactive puncta present in this structure, it was difficult to discern these immunoreactive neurons.

Densely stained neurons and neuropil were observed in the ventral tegmental nucleus (Fig. 5*A*) and in the gigantocellular reticular area (Fig. 5*B*). Both the cell bodies and dendritic processes of these large neurons were densely stained.

In the nucleus of the trapezoid body, intense immunoreactivity was observed in neuronal cell bodies and their processes (Fig. 5*C*). In the superior olivary complex (Fig. 5*C*), a dense plexus of immunoreactive axons was visible in the medial superior olivary nucleus as well as in the lateral superior olivary nucleus. Neuronal cell bodies and their dendrites were also stained throughout the superior olivary nuclei. Densely labeled neurons were also visible in the lateral reticular nucleus (Fig. 3*H*).

Several of the cranial nerve nuclei exhibited dense pp60$^{c\text{-}src(+)}$ immunoreactivity. In the oculomotor nucleus, immunoreactive perikarya and dendritic processes were visible (data not shown). Intensely labeled neuronal cell bodies were observed in the mesencephalic trigeminal nucleus (Fig. 6*A*). The spinal trigeminal nucleus also contained many pp60$^{c\text{-}src(+)}$-immunoreactive cells, as well as clusters of immunoreactive puncta (Fig. 6*B*). Immunoreactive perikarya, dendrites, and axons were visible in the facial nucleus (data not shown). In the cochlear nuclei, pp60$^{c\text{-}src(+)}$-immunoreactive neurons were differentially distributed, with the dorsal subdivision containing a greater number of labeled cells than the ventral subdivision (Fig. 3*G*).

Cerebellum

The cerebellum contained some of the most intensely labeled neurons in the brain. pp60$^{c\text{-}src(+)}$ immunoreactivity was localized to the cell body and dendritic processes of Purkinje cell neurons as well as in the cell bodies of granule cells (Fig. 7*A*). At high magnification, dense labeling of the dendritic processes of Purkinje cells was visible in the molecular layer of the cerebellar cortex (Fig. 7*B*). Proximal as well as distal segments of the Purkinje dendritic arbor were immunoreactive. All of the deep cerebellar nuclei contained substantial populations of immunoreactive neurons (Figs. 3*G*, 7*C*) in addition to immunoreactive axons, as indicated by the punctate nature of the labeling (Fig. 7*C*).

Mesencephalon

In the substantia nigra (Fig. 8*A*), pp60$^{c\text{-}src(+)}$ immunoreactivity was restricted to the cell bodies and dendrites of neurons in the pars reticulata and the pars lateralis with no significant staining of neurons in the substantia nigra pars compacta. The immunoreactive neurons in the substantia nigra pars reticulata had diverse morphologies. Some neurons were small and ovoid whereas others were large and fusiform. The neuropil in the substantia nigra pars reticulata was also labeled, indicative of immunoreactive dendrites and axons. In the substantia nigra pars lateralis, small clusters of immunoreactive neurons were visible. Dorsal to the substantia nigra, intense immunoreactivity was also observed in the large neurons of the red nucleus (Fig. 8*B*).

Diencephalon

Lightly stained pp60$^{c\text{-}src(+)}$-immunoreactive neurons were scattered throughout diencephalic structures, including portions of the mammillary body, lateral geniculate and reticular thalamic nuclei, zona incerta, and lateral hypothalamus (Fig. 3, *C, D*). Intensely immunoreactive neurons were rarely seen in these brain regions, except for the mammillary nucleus, where a moderate population of densely stained neurons was visible (data not shown).

Telencephalon

The major telencephalic region exhibiting intensely labeled pp60$^{c\text{-}src(+)}$-immunoreactive neurons was the cerebral cortex,

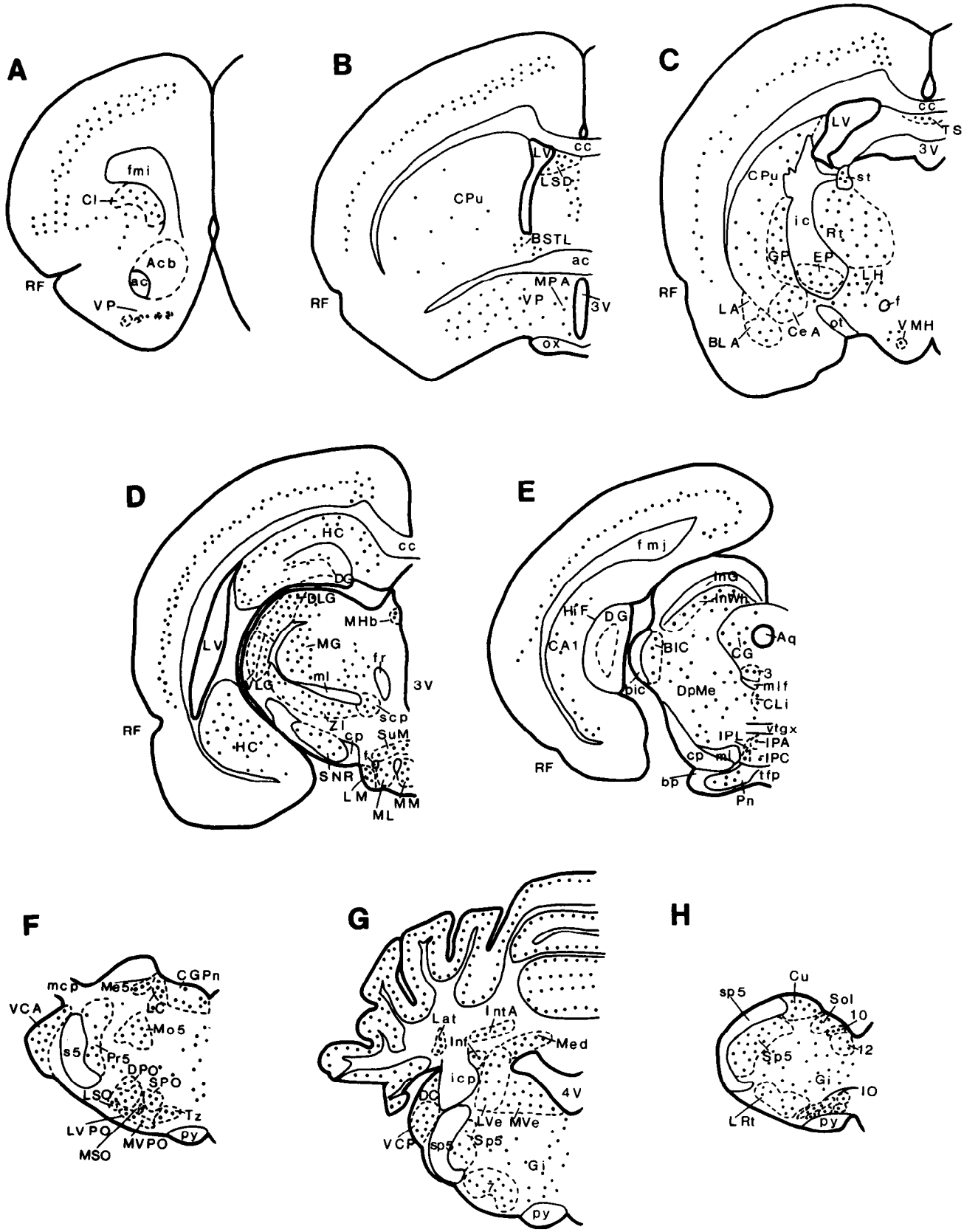

Figure 3. Schematic diagrams of half-coronal sections through the rat brain demonstrating the distribution of pp60$^{c\text{-}src(+)}$-containing neurons. Immunoreactive cell bodies have been indicated as *dots*. Each *dot* represents approximately 5 cells. In *G*, the dots in the top half of the drawing represent Purkinje cell neurons in the cerebellar cortex. The granule cells in the cerebellar cortex were also immunoreactive but are not indicated with *dots* on the upper part of the diagram due to the lack of space. See list of abbreviations in Appendix.

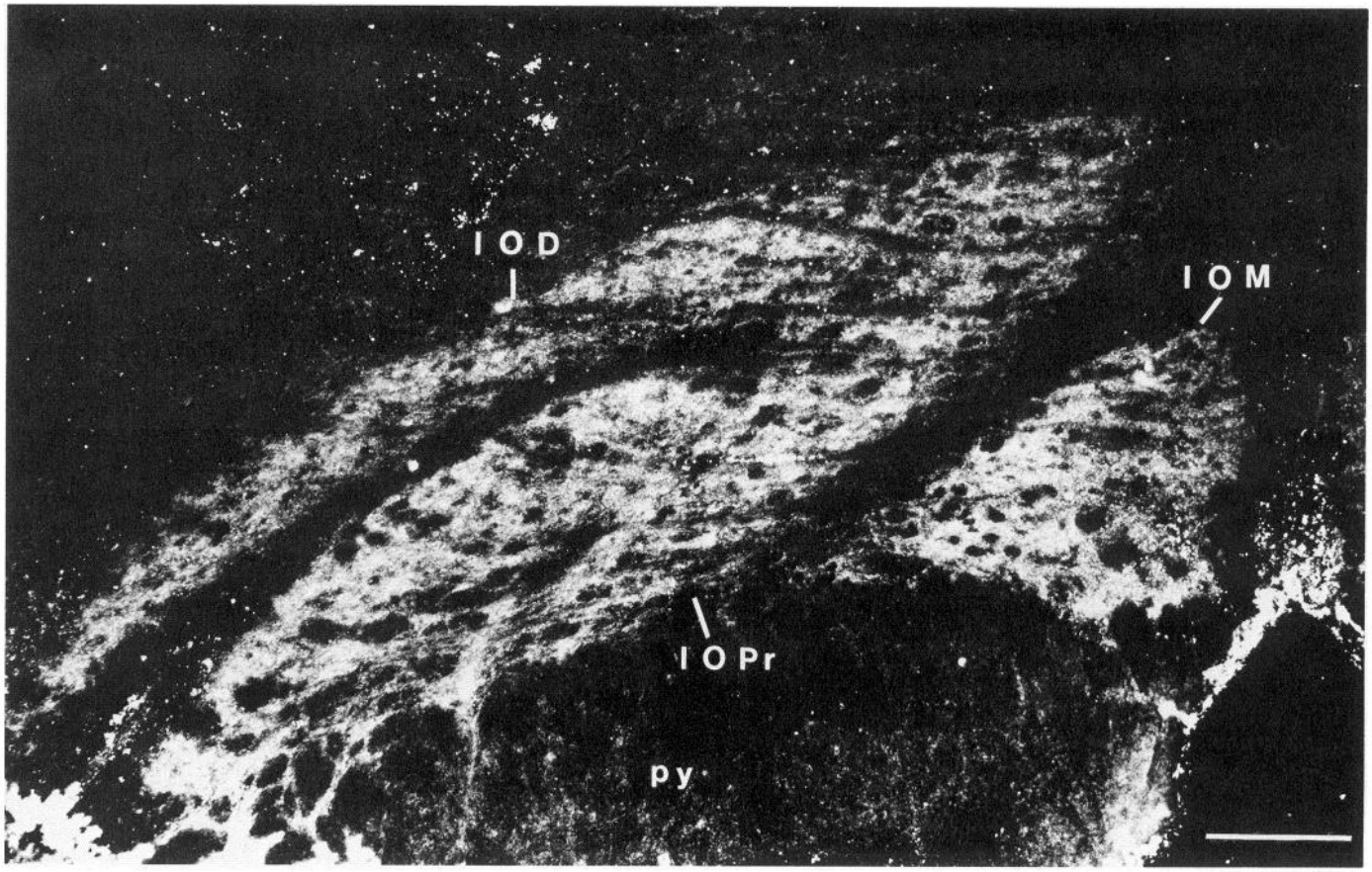

Figure 4. Dark-field photomicrograph showing pp60$^{c\text{-}src(+)}$ immunoreactivity in a coronal section through the inferior olive. Dense immunoreactive puncta were observed throughout the inferior olivary complex. Medial is to the right. *IOD,* Inferior olive, dorsal nucleus; *IOM,* inferior olive, medial nucleus; *IOPr,* inferior olive, principal nucleus; *py,* pyramidal tract. Scale bar, 100 μm.

where a distinct laminar organization was evident. In most areas of the cerebral cortex, only pyramidal neurons in layer V were densely labeled. Pyramidal neurons in layer VI of cortex were only lightly labeled. pp60$^{c\text{-}src(+)}$ immunoreactivity was localized within the cell bodies and dendritic processes of pyramidal neurons in layer V of the cerebral cortex (Fig. 9*A*). The apical and basilar dendritic processes of these immunoreactive neurons were also heavily labeled (Fig. 9*B*). One exception to this layer-specific localization pattern was observed in the insular cortex where pp60$^{c\text{-}src(+)}$ immunoreactivity was distributed throughout all layers (data not shown). No significant immunoreactivity was detected in the cerebral cortex ventral to the rhinal fissure (Fig. 3, *A–E*).

A substantial population of pp60$^{c\text{-}src(+)}$-immunoreactive neurons was also evident in the ventral pallidum, where the number of labeled neurons increased in the caudal direction (Fig. 3, *A, B*). In addition to perikaryal and dendritic localization of pp60$^{c\text{-}src(+)}$, a dense plexus of immunoreactive axons was also present in the ventral pallidum (Fig. 9, *C, D*). A moderate level of pp60$^{c\text{-}src(+)}$ immunoreactivity was visible in the pyramidal neurons in fields CA1–CA3 of the hippocampus (Fig. 10). The remainder of the telencephalic structures contained scattered, lightly immunoreactive neurons. These areas include caudate-putamen, globus pallidus, septum, and the central and basolateral amygdaloid nuclei (Fig. 3, *B, C*).

Discussion

We have described the distribution of the neuron-specific form of the c-*src* gene product, pp60$^{c\text{-}src(+)}$, in adult rat brain using an affinity-purified anti-peptide antibody that exclusively recognizes this variant form of c-*src* protein. These results confirm the neuronal specificity of pp60$^{c\text{-}src(+)}$, which was previously indicated by indirect studies in cultured cells (Brugge et al., 1985), neurological mutant mice (Brugge et al., 1987b), and neurochemical lesion studies (Walaas et al., 1988). Furthermore, this study represents the first report of pp60$^{c\text{-}src(+)}$ expression at the cellular level using immunocytochemistry.

The distribution of pp60$^{c\text{-}src(+)}$ was widespread yet restricted

→

Figure 5. pp60$^{c\text{-}src(+)}$ immunoreactivity in coronal sections through the brain stem. *A,* High magnification of the ventral tegmental nucleus. Neuronal cell bodies and neuropil are densely labeled. Medial is to the left. *B,* Low magnification of the gigantocellular reticular area. The cell bodies as well as the dendritic processes of these large neurons are intensely immunoreactive. Medial is to the left. *C,* Low magnification of the superior olivary complex and the nucleus of the trapezoid body. In the superior olivary complex, a dense plexus of immunoreactive axons (puncta) was observed

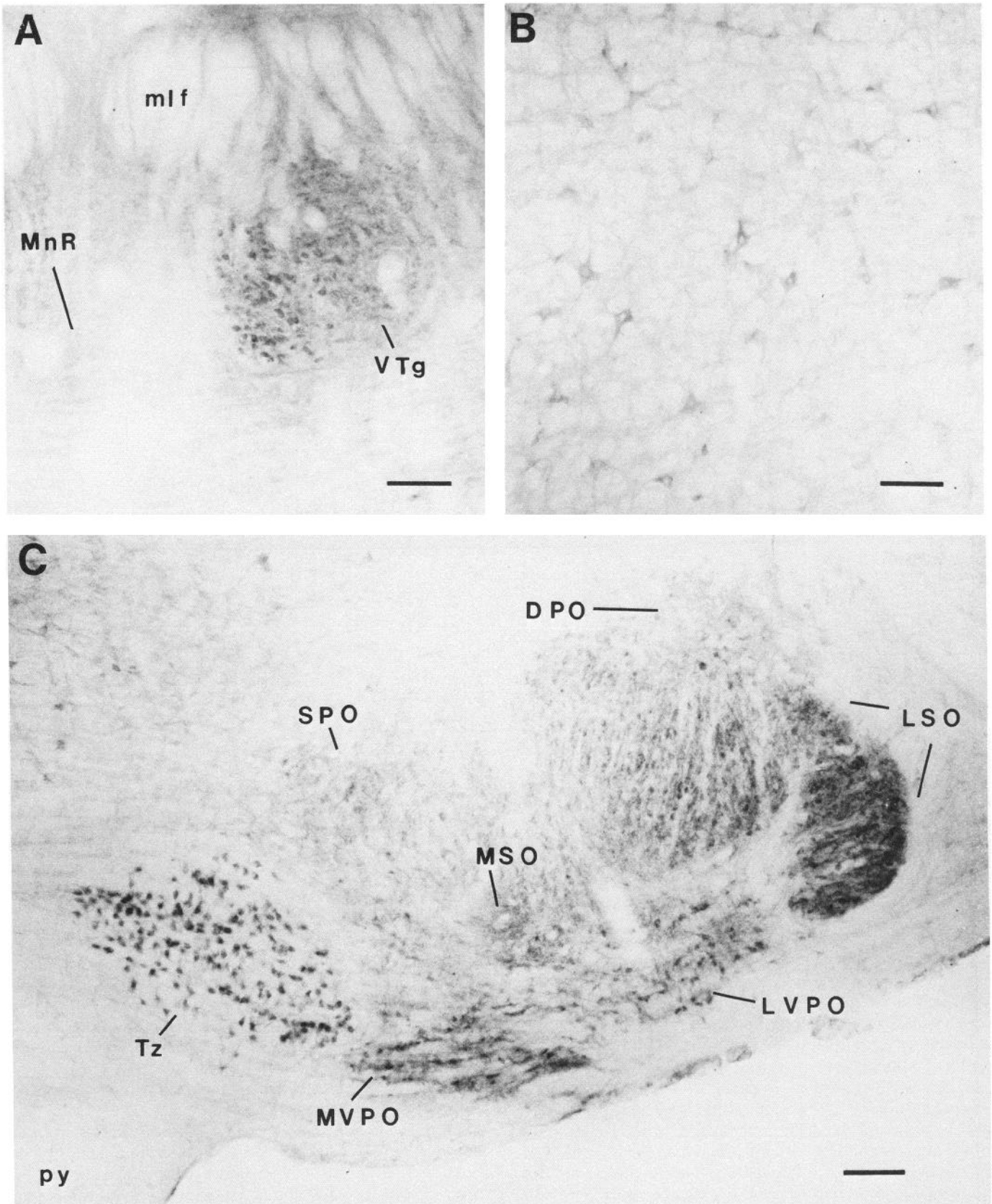

in the medial superior olivary nucleus as well as in the lateral superior olivary nucleus. Neuronal cell bodies and their dendrites were also labeled throughout the superior olivary nuclei. Medial is to the left. Scale bars, 100 μm. *DPO,* Dorsal periolivary region; *LSO,* lateral superior olive; *LVPO,* lateroventral periolivary nucleus; *mlf,* medial longitudinal fasciculus; *MnR,* median raphe nucleus; *MSO,* medial superior olive; *MVPO,* medioventral periolivary nucleus; *py,* pyramidal tract; *SPO,* superior paraolivary nucleus; *Tz,* nucleus of the trapezoid body; *VTg,* ventral tegmental nucleus.

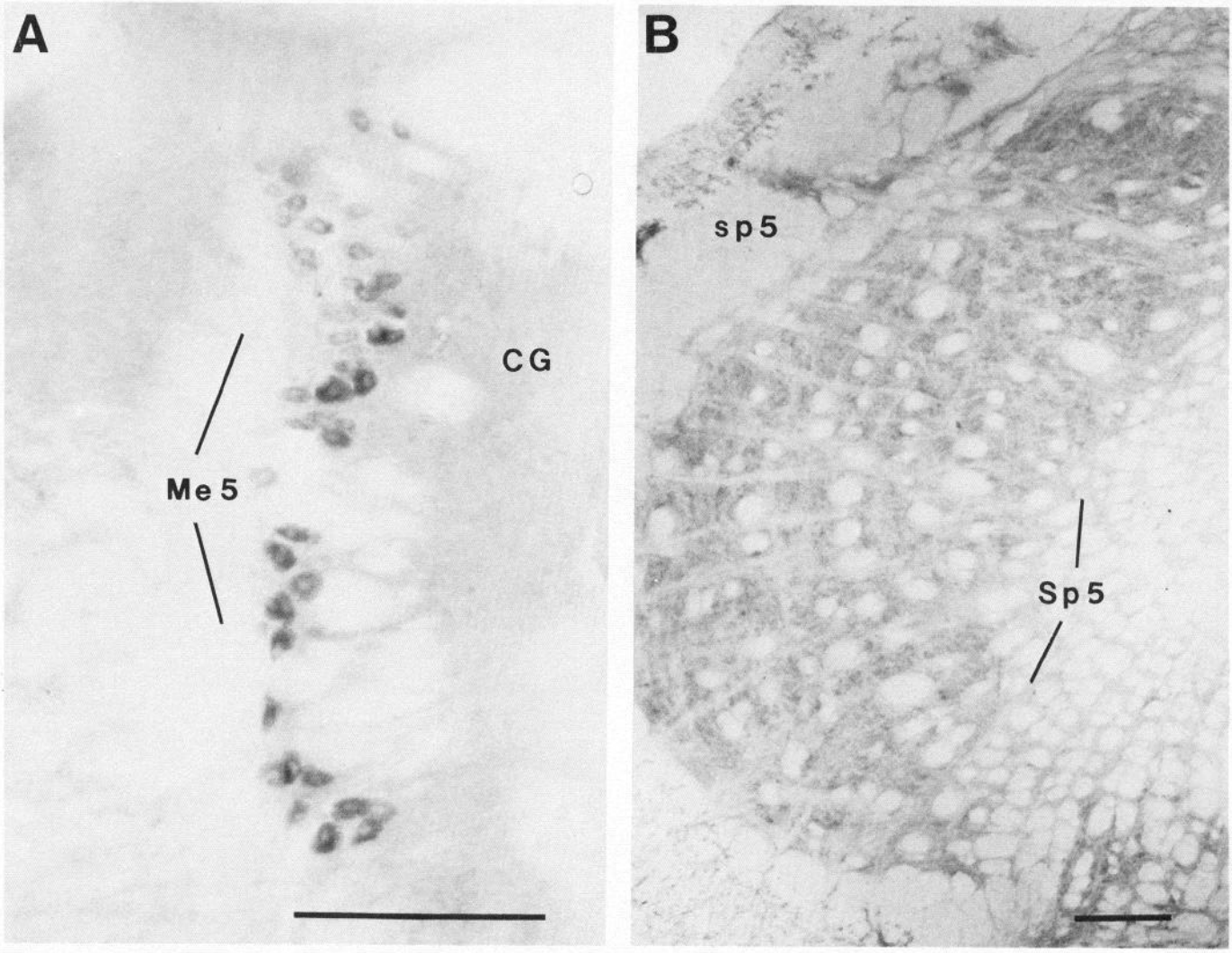

Figure 6. pp60$^{c\text{-}src(+)}$ immunoreactivity in coronal sections through cranial nerve nuclei in the brain stem. *A,* High magnification of the mesencephalic trigeminal nucleus. Note the intense immunoreactivity in the cell bodies of these large neurons. Medial is to the right. *B,* Low magnification of the spinal trigeminal nucleus. Dense clusters of immunoreactive puncta were visible. Neuronal cell bodies were also densely labeled. Medial is to the right. Scale bars, 200 μm. *CG,* Central gray; *Me5,* mesencephalic trigeminal nucleus; *sp5,* spinal trigeminal tract; *Sp5,* spinal trigeminal nucleus.

in the rat brain. pp60$^{c\text{-}src(+)}$ was not detected in all neuronal cells, but rather appears to be differentially expressed in subpopulations of neurons throughout the rat brain. Thus, pp60$^{c\text{-}src(+)}$ does not appear to be restricted to specific classes of neurons that share an obvious common feature, such as morphology, neurotransmitter responsiveness, or neurotransmitter/neuropeptide localization.

At the subcellular level, the distribution of pp60$^{c\text{-}src(+)}$ was also widespread. pp60$^{c\text{-}src(+)}$ immunoreactivity was localized within the cell body and dendritic processes of certain neurons. In several discrete areas of the brain, including the inferior olive, superior olive, and spinal trigeminal nucleus, pp60$^{c\text{-}src(+)}$ immunoreactivity was also localized to axons and nerve terminals as demonstrated by the presence of immunoreactive puncta. The localization of pp60$^{c\text{-}src(+)}$ within these functionally important areas of the neuron suggests that this unique form of the c-*src* gene product may serve a regulatory role in multiple nerve cell functions.

The analysis of a closely related protein, pp56^{lck}, which is structurally homologous to pp60$^{c\text{-}src(+)}$ has shed some light on the potential functions of this class of membrane-bound tyrosine protein kinases. This T-cell-specific protein is structurally and functionally coupled to the CD4/CD8 membrane proteins, which serve as receptors for the major histocompatibility antigens (Veillette et al., 1988, 1989). By analogy, pp60$^{c\text{-}src(+)}$ may associate with and be regulated by a neuronal cell receptor protein. However, the pattern of expression of pp60$^{c\text{-}src(+)}$ in the adult brain does not appear to correlate with the expression of any known receptor protein molecule. Furthermore, pp60$^{c\text{-}src(+)}$ has been detected throughout the nerve cell: in the cell body, dendritic processes, axons, and nerve terminals. In addition, membrane fractionation studies have indicated that pp60$^{c\text{-}src(+)}$ is enriched in synaptic vesicles in adult rat brain (Pang et al., 1988a, b) as well as in growth cones of developing neurons (Maness et al., 1988). These results suggest a more generalized function for pp60$^{c\text{-}src(+)}$ in neurons.

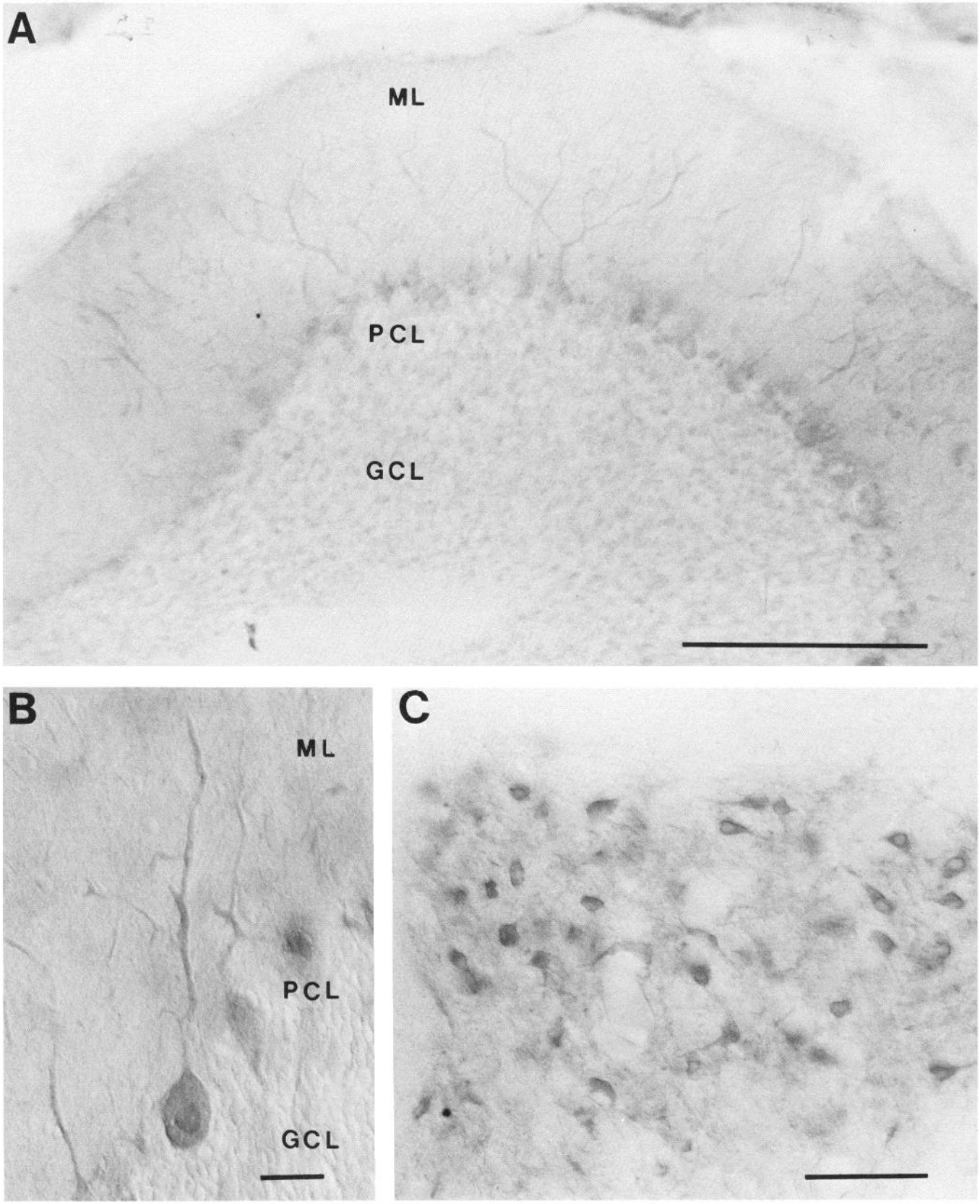

Figure 7. pp60$^{c\text{-}src(+)}$ immunoreactivity in coronal sections through the cerebellum. *A,* Low magnification of the cerebellar cortex. pp60$^{c\text{-}src(+)}$ immunoreactivity was localized within the cell bodies and dendritic processes of Purkinje cell neurons as well as in the cell bodies of granule cells. In the molecular layer of the cerebellar cortex, dense labeling was observed in proximal as well as distal segments of the Purkinje cell dendritic arbor. Medial is to the left. Scale bar, 100 μm. *B,* High magnification of a Purkinje cell neuron. Note the dense label in both the cell soma and the dendritic processes of this neuron. Scale bar, 20 μm. *C,* High magnification of the medial cerebellar nucleus. Dense pp60$^{c\text{-}src(+)}$ immunoreactivity was visible in neuronal cell bodies and dendritic processes in the deep cerebellar nuclei. Immunoreactive puncta were also observed in all of the deep cerebellar nuclei. Medial is to the right. Scale bar, 100 μm. *GCL,* Granule cell layer; *ML,* molecular layer; *PCL,* Purkinje cell layer.

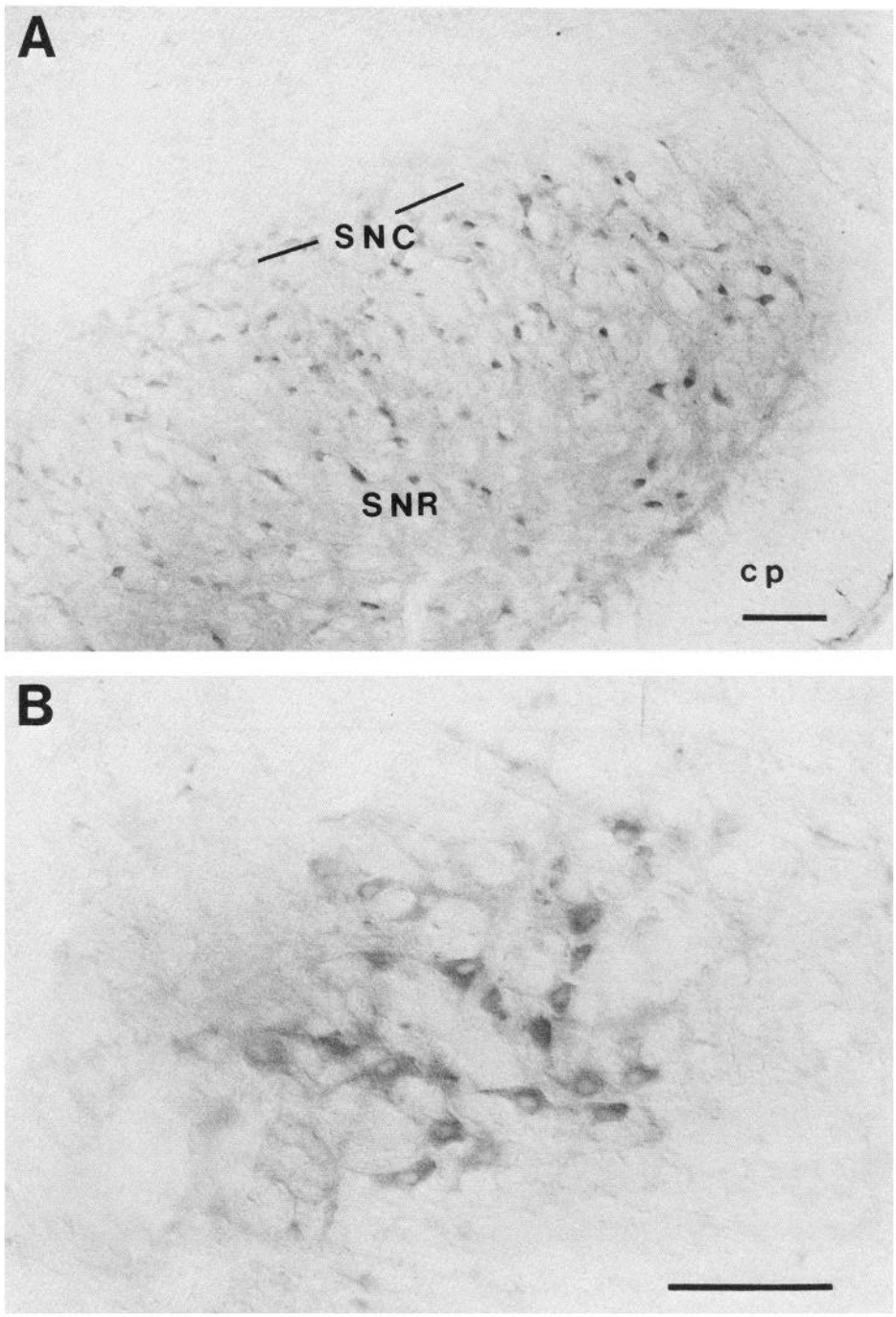

Figure 8. pp60$^{c\text{-}src(+)}$ immunoreactivity in coronal sections through the substantia nigra (*A*) and the red nucleus (*B*). *A*, High magnification of the substantia nigra. Note the dense labeling of neuronal cell bodies and dendrites in the substantia nigra reticulata. The neuropil in the substantia nigra reticulata was also labeled, indicative of immunoreactive dendrites and axons. No significant staining of neurons was visible in the substantia nigra compacta. Medial is to the left. *B*, High magnification of the red nucleus. Note the intense immunoreactivity localized to the cell body and dendritic processes of these large neurons. Medial is to the right. Scale bars, 100 μm. *cp*, Cerebral peduncle, basal; *SNC*, substantia nigra compacta; *SNR*, substantia nigra reticulata.

Our results confirm and extend previous c-*src*(+) localization studies. Recently, an *in situ* hybridization study showed that c-*src*(+) mRNA was localized to neuronal cell bodies using a specific oligonucleotide probe (Ross et al., 1988). In general, the immunocytochemical distribution of pp60$^{c\text{-}src(+)}$ is similar to the pattern observed in the *in situ* studies; however, the regional distribution of c-*src*(+) mRNA was slightly different from the pattern of expression of pp60$^{c\text{-}src(+)}$ we report here. While the *in*

→

Figure 9. pp60$^{c\text{-}src(+)}$ immunoreactivity in coronal sections through the cerebral cortex (*A*, *B*) and the ventral pallidum (*C*, *D*). *A*, Low magnifications of the cerebral cortex. A distinct laminar organization was evident in the cerebral cortex. Note the dense immunoreactivity in pyramidal neurons of layer V of the hindlimb area of cortex. This pattern of staining was observed in most areas of the cerebral cortex. Pyramidal neurons in layer VI were only lightly labeled. Medial is to the right. Scale bar, 200 μm. *B*, High magnification of a pyramidal neuron in layer V of temporal cortex. pp60$^{c\text{-}src(+)}$ immunoreactivity was localized within the cell body and dendritic processes of this pyramidal neuron. Note the dense labeling of both the apical and basilar dendritic processes. Scale bar, 20 μm. *C*, Low magnification of the ventral pallidum. Dense pp60$^{c\text{-}src(+)}$ immunoreactivity was observed in cell bodies and dendrites in the ventral pallidum. Medial is to the left. Scale bar, 100 μm. *D*, High magnification of the ventral pallidum. Note the dense plexus of immunoreactive axons. Medial is to the left. Scale bar, 100 μm. *Tu*, Olfactory tubercle; *VP*, ventral pallidum.

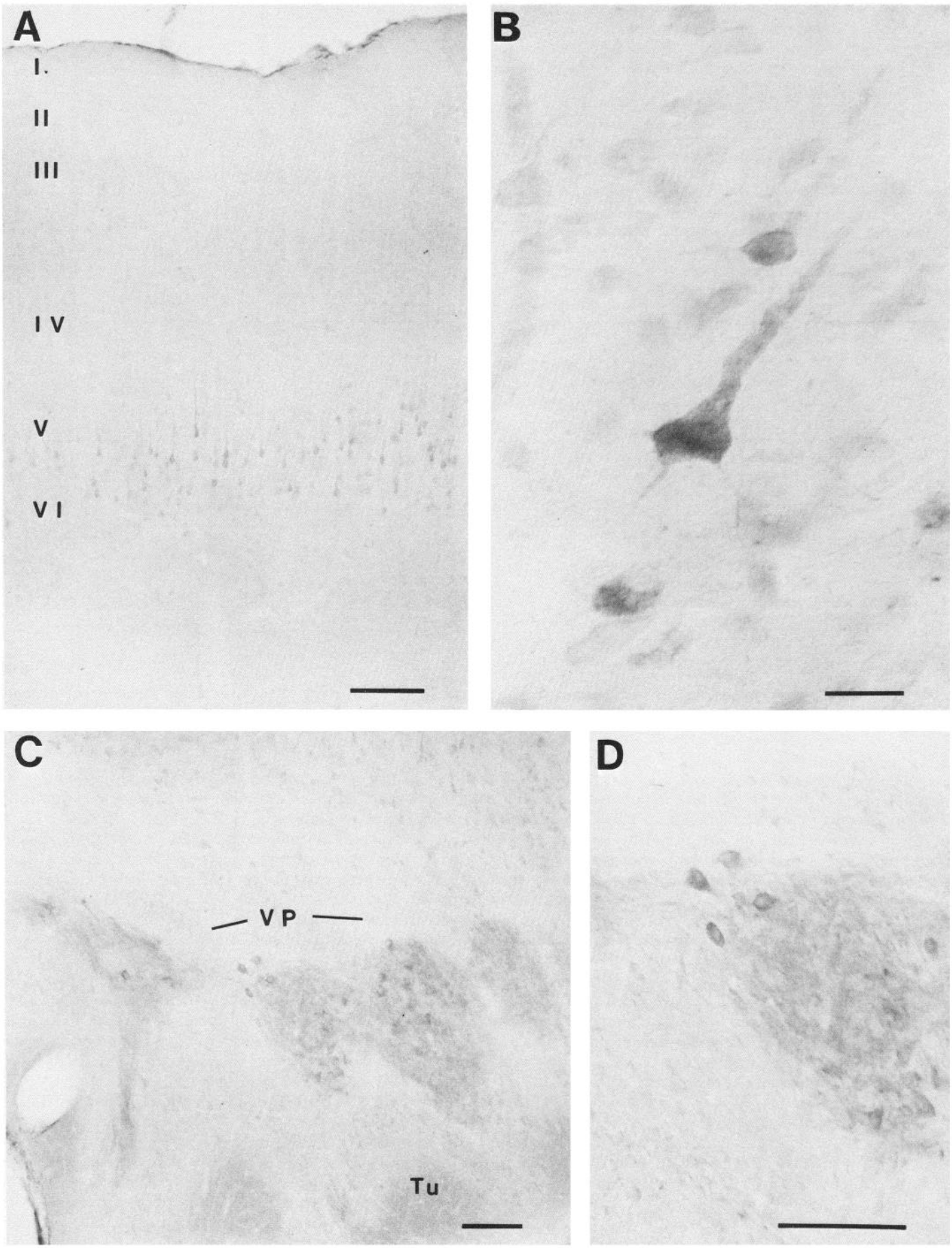
A
I
II
III
IV
V
VI
B
C
VP
Tu
D

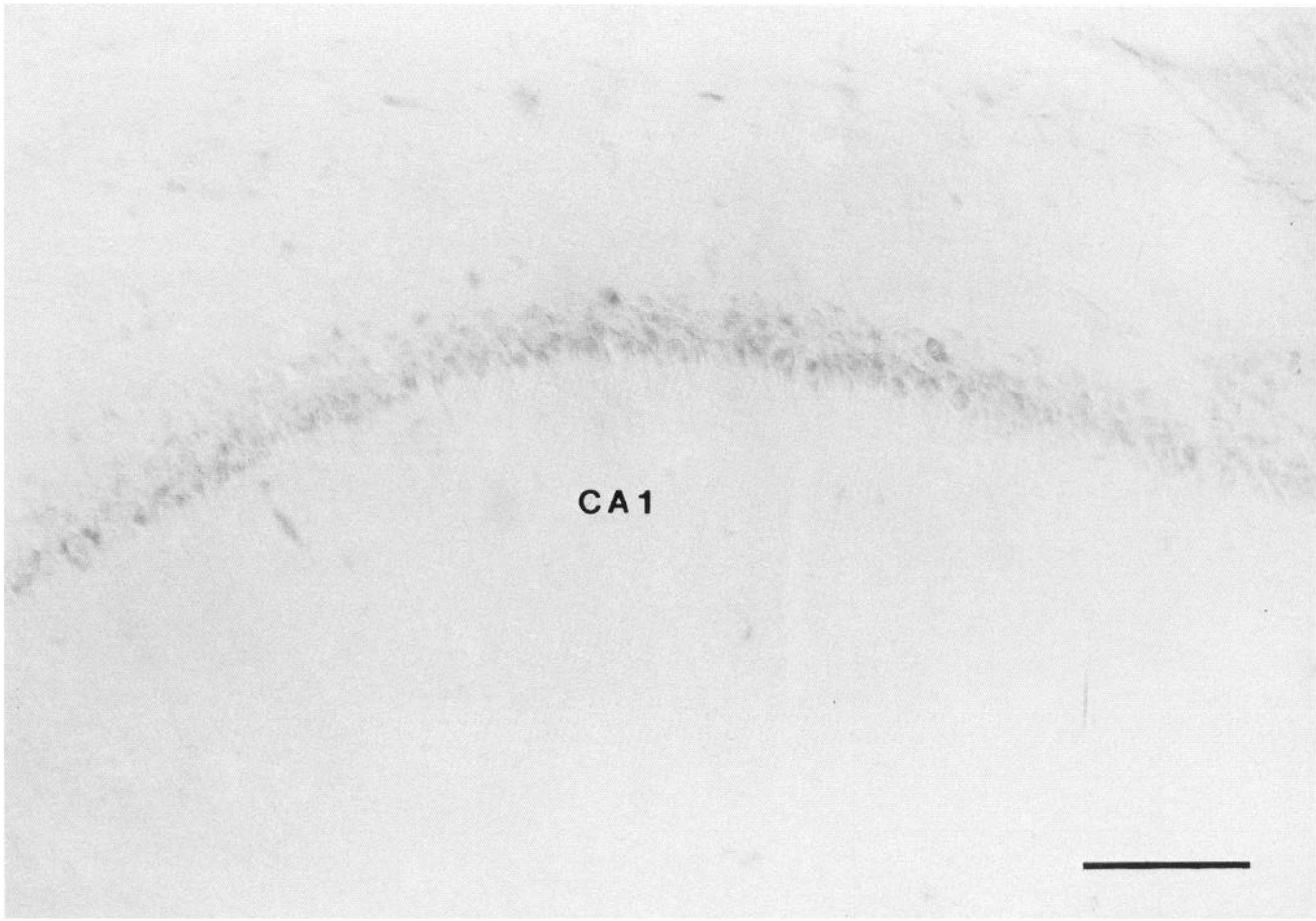

Figure 10. pp60$^{c\text{-}src(+)}$ immunoreactivity in a coronal section through the hippocampus. Moderately labeled neurons were visible in the CA1 region of the hippocampus. Medial is to the left. Scale bar, 100 μm.

situ studies showed very high levels of probe binding in the hippocampus, we observed only moderate levels of pp60$^{c\text{-}src(+)}$ immunoreactivity in this structure (Fig. 10). Biochemical studies also indicate that high levels of c-*src*(+) protein are expressed in the hippocampus (Ross et al., 1988; Walaas et al., 1988). One possible explanation for this difference is that a moderate level of pp60$^{c\text{-}src(+)}$ may be expressed in most neurons of the hippocampus, which contains a high density of neurons. This would explain why the levels of pp60$^{c\text{-}src(+)}$ detected at the cellular level using immunocytochemistry appear lower than in biochemical assays in which the amount of pp60$^{c\text{-}src(+)}$ is assayed relative to total protein within a particular brain region.

Another difference between our immunocytochemical findings and previous results is that we observed some of the highest levels of pp60$^{c\text{-}src(+)}$ immunoreactivity in specific populations of cells within the brain stem, while the *in situ* hybridization study (Ross et al., 1988) and a previous biochemical study (Walaas et al., 1988) revealed low levels of c-*src*(+) mRNA and protein, respectively, in the pons and medulla. In those areas of the brain stem where we observed intense immunoreactive puncta, including the inferior and superior olive and the spinal trigeminal nucleus, one would not expect to see a similar pattern by *in situ* hybridization since mRNA is largely restricted to the cell bodies. Furthermore, in most biochemical studies the pons and medulla were homogenized together, thereby possibly preventing the detection of high levels of pp60$^{c\text{-}src(+)}$ expression in particular subnuclei in the brain stem.

Another member of the *src* family of tyrosine protein kinases has been shown to be expressed at high levels in the brain. Sudol et al. (1988) demonstrated that the proto-oncogene c-*yes* is expressed at high levels in the cerebellum, specifically in Purkinje cell neurons (Sudol et al., 1989). The dendritic processes of Purkinje cell neurons showed the most intense staining for pp62$^{c\text{-}yes}$, the c-*yes* protein, whereas the cell bodies were less densely labeled. Our results indicate that pp60$^{c\text{-}src(+)}$ is also expressed in Purkinje cells. Dense pp60$^{c\text{-}src(+)}$ immunoreactivity was localized to cell bodies, dendritic processes, and axons of Purkinje cells in the rat cerebellum (Fig. 7). It is interesting that 2 such closely related proto-oncogenes are co-localized in one particular neuronal cell type. Perhaps each of these tyrosine-specific protein kinases is involved in the regulation of distinct processes. Unlike the c-*yes* protein, which is expressed at high levels in many different tissues, including brain, liver, kidney, and gonads, pp60$^{c\text{-}src(+)}$ is expressed exclusively in neurons. Therefore, it is possible that pp60$^{c\text{-}src(+)}$ may serve a neuron-specific function, whereas pp62$^{c\text{-}yes}$ may regulate a more general cellular function. Studies aimed at defining the precise subcellular localization of pp60$^{c\text{-}src(+)}$ and pp62$^{c\text{-}yes}$ should yield further

information regarding the physiological significance of these tyrosine kinases in the Purkinje cell neuron.

Our immunocytochemical results indicate that pp60$^{c\text{-}src(+)}$ was present at high levels in nerve terminals located in the inferior olive, superior olive, and spinal trigeminal nucleus, whereas low levels of pp60$^{c\text{-}src(+)}$ immunoreactivity were detected in nerve terminals in several brain regions, including the substantia nigra. Other evidence for the localization of pp60$^{c\text{-}src(+)}$ in nerve terminals comes from deafferentation studies in which a significant loss of the c-*src*(+) protein was detected in the substantia nigra following lesions that interrupted afferent fibers coming from the neostriatum (Walaas et al., 1988). Previously, it was shown that synaptic vesicle proteins are phosphorylated by endogenous tyrosine kinases, and that pp60$^{c\text{-}src}$ is expressed in nerve terminals and crude synaptic vesicle fractions (Pang et al., 1988a). More recently, Pang et al. (1988b) demonstrated that pp60$^{c\text{-}src(+)}$ is present at high levels in purified synaptic vesicles. Furthermore, pp60$^{c\text{-}src(+)}$ was the most abundant tyrosine-specific protein kinase in synaptic vesicles. Together these studies suggest that pp60$^{c\text{-}src(+)}$ may play a role in signal transduction at the nerve terminal.

In summary, the widespread distribution of pp60$^{c\text{-}src(+)}$ in diverse neuronal cell types suggests the existence of a previously uncharacterized functional organization within the brain. The localization of this neuron-specific tyrosine kinase in functionally important areas of the nerve cell, namely dendrites, axons, and nerve terminals, suggests that pp60$^{c\text{-}src(+)}$ may regulate pleiotropic functions in specific classes of neurons in the adult central nervous system. Studies aimed at examining the developmental expression of pp60$^{c\text{-}src(+)}$ will provide further clues as to the physiological importance of this proto-oncogene in neurons. It will also be important to compare the cellular and subcellular distribution of the multiple members of the *src* family of tyrosine kinases that are expressed in the brain to obtain clues to the specific functions of these tyrosine kinases in the central nervous system.

Appendix

Abbreviations

3,	oculomotor nucleus;
3V,	3rd ventricle;
7,	facial nucleus;
10,	vagus nucleus;
12,	hypoglossal nucleus;
ac,	anterior commissure;
Acb,	accumbens nucleus;
aq,	aqueduct (Sylvius);
bic,	brachium of the inferior colliculus;
BIC,	nucleus of the brachium of the inferior colliculus;
BLA,	basolateral amygdaloid nucleus, anterior part;
bp,	brachium pontis (stem of middle cerebellar peduncle);
BSTL,	bed nucleus of the stria terminalis, lateral division;
cc,	corpus callosum;
CeA,	central amygdaloid nucleus, anterior part;
CG,	central gray;
CGPn,	central gray of the pons;
Cl,	claustrum;
Cli,	caudal linear nucleus of the raphe;
cp,	cerebral peduncle;
CPu,	caudata putamen;
Cu,	cuneate nucleus;
DC,	dorsal cochlear nucleus;
DG,	dentate gyrus;
DLG,	dorsal lateral geniculate nucleus;
DpMe,	deep mesencephalic nucleus;
DPO,	dorsal periolivary region;
EP,	entopeduncular nucleus;
f,	fornix;
fmj,	forceps major of the corpus callosum;
fr,	fasciculus retroflexus;
Gi,	gigantocellular reticular area;
GP,	globus pallidus;
HC,	hippocampus;
HiF,	hippocampal fissure;
ic,	internal capsule;
Inf,	infracerebellar nucleus;
InG,	intermediate gray layer of the superior colliculus;
IntA,	interposed cerebellar nucleus;
InWh,	intermediate white layer of the superior colliculus;
IO,	inferior olive;
IPA,	interpeduncular nucleus, apical subnucleus;
IPC,	interpeduncular nucleus, caudal subnucleus;
IPL,	interpeduncular nucleus, dorsomedial subnucleus;
LA,	lateroanterior hypothalamic nucleus;
Lat,	lateral cerebellar nucleus;
LC,	locus coeruleus;
LH,	lateral hypothalamic area;
LM,	lateral mammillary nucleus;
LRt,	lateral reticular nucleus;
LSD,	lateral septal nucleus, dorsal part;
LSO,	lateral superior olive;
LV,	lateral ventricle;
LVe,	lateral vestibular nucleus;
LVPO,	lateroventral periolivary nucleus;
mcp,	medial cerebellar peduncle;
Me5,	mesencephalic trigeminal nucleus;
Med,	medial cerebellar nucleus;
MG,	medial geniculate nucleus;
MHb,	medial habenular nucleus;
ML,	medial mammillary nucleus, lateral part;
ml,	medial lemniscus;
MM,	medial mammillary nucleus, medial part;
Mo5,	motor trigeminal nucleus;
MPA,	medial preoptic area;
MSO,	medial superior olive;
MVe,	medial vestibular nucleus;
MVPO,	medioventral periolivary nucleus;
ot,	optic tract;
ox,	optic chiasm;
Pn,	pontine nuclei;
Pr5,	principal sensory trigeminal nucleus;
py,	pyramidal tract;
RF,	rhinal fissure;
Rt,	reticular thalamic nucleus;
s5,	sensory root of the trigeminal nerve;
scp,	superior cerebellar peduncle;
SNR,	substantia nigra reticular part;
Sol,	nucleus of the solitary tract;
sp5,	spinal trigeminal tract;
Sp5,	spinal trigeminal nucleus;
SPO,	superior paraolivary nucleus;
st,	stria terminalis;
SuM,	supramammillary nucleus;
tfp,	transverse fibers of the pons;
TS,	triangular septal nucleus;
Tz,	nucleus of the trapezoid body;
VCA,	ventral cochlear nucleus, anterior part;
VCP,	ventral cochlear nucleus, posterior part;
VLG,	ventral lateral geniculate nucleus;
VMH,	ventromedial hypothalamic nucleus;
VP,	ventral pallidum;
vtgx,	ventral tegmental decussation; and
ZI,	zona incerta.

References

Anderson SK, Gibbs CP, Tanaka A, Kung H-J, Fujita DJ (1985) Human cellular *src* gene: nucleotide sequence and derived amino acid sequence of the region coding for the carboxy-terminal two-thirds of pp60$^{c\text{-}src}$. Mol Cell Biol 5:1122–1129.

Barany G, Merrifield RB (1979) Solid phase peptide synthesis. In: The

peptides: analysis, synthesis, biology (Gross E, Meienhofer J, eds), pp 137–145. New York: Academic.

Barnekow A, Schartl M (1984) Cellular *src* gene product detected in the freshwater sponge *Spongilla lacustris*. Mol Cell Biol 4:1179–1181.

Barnekow A, Schartl M, Anders F, Bauer H (1982) Identification of a fish protein associated with a kinase activity and related to the Rous sarcoma virus transforming protein. Cancer Res 42:2429–2433.

Bishop JM (1983) Cellular oncogenes and retroviruses. Annu Rev Biochem 52:301–304.

Bolen JB, Rosen N, Israel MA (1985) Increased pp60$^{c\text{-}src}$ tyrosyl kinase activity in human neuroblastomas is associated with amino-terminal tyrosine phosphorylation of the *src* gene product. Proc Natl Acad Sci USA 82:7275–7279.

Bolen JB, Veillette A, Schwartz AM, Deseau V, Rosen N (1987) Analysis of pp60$^{c\text{-}src}$ in human colon carcinoma and normal human colon mucosal cells. Oncogene Res 1:149–168.

Brugge JS, Cotton PC, Queral AE, Barrett JN, Nonner D, Keane RW (1985) Neurones express high levels of a structurally modified, activated form of pp60$^{c\text{-}src}$. Nature (Lond) 316:554–557.

Brugge J, Cotton P, Lustig A, Yonemoto W, Lipsich L, Coussens P, Barrett JN, Nonner D, Keane RW (1987a) Characterization of the altered form of the c-*src* gene product in neuronal cells. Genes Dev 1:287–296.

Brugge JS, Lustig A, Messer A (1987b) Changes in the pattern of expression of pp60$^{c\text{-}src}$ in cerebellar mutants of mice. J Neurosci Res 18:532–538.

Cartwright CA, Simantov R, Kaplan PL, Hunter T, Eckhart W (1987) Alterations in pp60$^{c\text{-}src}$ accompany differentiation of neurons from rat embryo striatum. Mol Cel Biol 7:1830–1840.

Cartwright CA, Simantov R, Cowan WM, Hunter T, Eckhart W (1988) pp60$^{c\text{-}src}$ expression in the developing rat brain. Proc Natl Acad Sci USA 85:3348–3352.

Cooper JA (1989) The *src*-family of protein-tyrosine kinases. In: Peptides and protein phosphorylation (Kemp B, Alewood PF, eds). Boca Raton, FL: CRC (in press).

Cotton PC, Brugge JS (1983) Neural tissues express high levels of the cellular *src* gene product pp60$^{c\text{-}src}$. Mol Cell Biol 3:1157–1162.

Fults DW, Towle AC, Lauder JM, Maness PF (1985) pp60$^{c\text{-}src}$ in the developing cerebellum. Mol Cell Biol 5:27–32.

Gessler M, Barnekow A (1984) Differential expression of the cellular oncogene c-*src* and c-*yes* in embryonal and adult chicken tissues. Biosci Rep 4:757–770.

Golden A, Brugge JS (1988) The *src* oncogene. In: The oncogene handbook (Reddy EP, Curran T, Skalka A, eds), pp 149–173. Cambridge UK: Elsevier.

Gregory RJ, Kammermeyer KL, Vincent WS, III, Wadsworth SG (1987) Primary sequence and developmental expression of a novel *Drosophila melanogaster src* gene. Mol Cell Biol 7:2119–2127.

Hoffman-Falk H, Einat P, Shilo B-Z, Hoffman FM (1983) *Drosophila melanogaster* DNA clones homologous to vertebrate oncogenes: evidence for a common ancestor to the *src* and *abl* cellular genes. Cell 32:589–598.

Hsu S-M, Raine L, Fanger H (1981) Use of avidin-biotin-peroxidase complex (ABC) in immunoperoxidase techniques: a comparison between ABC and unlabeled antibody (PAP) procedures. J Histochem Cytochem 29:577–580.

Hughes SH, Greenhouse JJ, Petropoulos CJ, Sutrave P (1987) Adaptor plasmids simplify the insertion of foreign DNA into helper-independent retroviral vectors. J Virol 61:3004–3012.

Hunter T, Cooper JA (1985) Protein-tyrosine kinases. Annu Rev Biochem 54:897–930.

Kagan A, Glick SM (1979) Oxytocin II. Methods of radioimmunoassay. In: Methods of hormone radioimmunoassay (Jaffe BM, Behrman HR, eds), pp 328–329. New York: Academic.

Laemmli UK (1970) Cleavage of structural proteins during the assembly of the head of bacteriophage T4. Nature (Lond) 227:680–685.

LeBeau JM, Wiestler OD, Walter G (1987) An altered form of pp60$^{c\text{-}src}$ is expressed primarily in the central nervous system. Mol Cell Biol 7:4115–4117.

Levy BT, Sorge LK, Meymandi A, Maness PF (1984) pp60$^{c\text{-}src}$ kinase is in chick and human embryonic tissues. Dev Biol 104:9–17.

Levy JB, Brugge JS (1989) Biological and biochemical properties of the c-*src*(+) gene product overexpressed in chick embryo fibroblasts. Mol Cell Biol 9:3332–3341.

Levy JB, Dorai T, Wang L-H, Brugge JS (1987) The structurally distinct form of pp60$^{c\text{-}src}$ detected in neuronal cells is encoded by a unique c-*src* mRNA. Mol Cell Biol 7:4142–4145.

Lipsich LA, Lewis AJ, Brugge JS (1983) Isolation of monoclonal antibodies that recognize the transforming proteins of avian sarcoma viruses. J Virol 48:352–360.

Lowry OH, Rosebrough NJ, Farr AL, Randall R (1951) Protein measurement with the Folin phenol reagent. J Biol Chem 193:265–275.

Lynch SA, Brugge JS, Levine JM (1986) Induction of altered c-*src* product during neural differentiation of embryonic carcinoma cells. Science 234:873–876.

Maness PF (1986) pp60$^{c\text{-}src}$ encoded by the proto-oncogene c-*src* is a product of sensory neurons. J Neurosci Res 16:127–139.

Maness PF, Sorge LK, Fults DW (1986) An early developmental phase of pp60$^{c\text{-}src}$ expression in the neural ectoderm. Dev Biol 117:83–89.

Maness PF, Aubry M, Shores CG, Frame L, Pfenninger KH (1988) c-*src* gene product in developing brain is enriched in nerve growth cone membranes. Proc Natl Acad Sci USA 85:5001–5005.

Martinez R, Mathey-Prevot B, Bernards A, Baltimore D (1987) Neuronal pp60$^{c\text{-}src}$ contains a six-amino acid insertion relative to its nonneuronal counterpart. Science 237:411–415.

Mellström K, Bjelfman C, Hammerling U, Påhlman S (1987) Expression of c-*src* in cultured human neuroblastoma and small-cell lung carcinoma cell lines correlates with neurocrine differentiation. Mol Cell Biol 7:4178–4184.

Pang DT, Wang JKT, Valtorta F, Benfenati F, Greengard P (1988a) Protein tyrosine phosphorylation in synaptic vesicles. Proc Natl Acad Sci USA 85:762–766.

Pang DT, Valtorta F, DeMarco ME, Brugge JS, Benfenati F, Greengard P (1988b) Localization of pp60$^{c\text{-}src}$ in synaptic vesicles. Soc Neurosci Abstr 14:44.6.

Pyper JM, Bolen JB (1989) Neuron-specific splicing of c-*src* RNA in human brain. J Neurosci Res 24:89–96.

Raulf F, Robertson SM, Schartl M (1989a) Evolution of the neuron-specific alternative splicing product of the c-*src* proto-oncogene. J Neurosci Res 24:81–88.

Raulf F, Mäueler W, Robertson SM, Schartl M (1989b) Localization of cellular *src* mRNA during development and in the differentiated bipolar neurons of the adult neural retina in *Xiphophorus*. Oncogene Res 5:39–47.

Rosenberg AH, Lade BN, Chui D-S, Lin S-W, Dunn JJ, Studier FW (1987) Vectors for selective expression of cloned DNAs by T7 RNA polymerase. Gene 56:125–135.

Ross CA, Wright GE, Resh MD, Pearson RCA, Snyder SH (1988) Brain-specific *src* oncogene mRNA mapped in rat brain by *in situ* hybridization. Proc Natl Acad Sci USA 85:9831–9835.

Schartl M, Barnekow A (1984) Differential expression of the cellular *src* gene during vertebrate development. Dev Biol 105:415–422.

Shilo B-Z, Weinberg RA (1981) DNA sequences homologous to vertebrate oncogenes are conserved in *Drosophila melanogaster*. Proc Natl Acad Sci USA 78:6789–6792.

Shores CG, Cox ME, Maness PF (1987) A tyrosine kinase related to pp60$^{c\text{-}src}$ is associated with membranes of *Electrophorus electricus* electric organ. J Biol Chem 262:9477–9485.

Simon MA, Kornberg TB, Bishop JM (1983) Three loci related to the *src* oncogene and tyrosine-specific protein kinase activity in *Drosophila*. Nature 302:837–839.

Simon MA, Drees B, Kornberg T, Bishop JM (1985) The nucleotide sequence and the tissue-specific expression of *Drosophila* c-*src*. Cell 42:831–840.

Sorge LK, Levy BT, Maness PF (1984) pp60$^{c\text{-}src}$ is developmentally regulated in the neural retina. Cell 36:249–257.

Sorge JP, Sorge LK, Maness PF (1985) pp60$^{c\text{-}src}$ is expressed in human fetal and adult brain. Am J Pathol 119:151–157.

Stehelin D, Varmus HE, Bishop JM, Vogt PK (1976) DNA related to the transforming gene(s) of avian sarcoma viruses is present in normal avian DNA. Nature 260:170–173.

Sudol M, Alvarez-Buylla A, Hanafusa H (1988) Differential developmental expression of cellular *yes* and cellular *src* proteins in cerebellum. Oncogene Res 2:345–355.

Sudol M, Kuo CF, Shigemitsu L, Alvarez-Buylla A (1989) Expression of the *yes* proto-oncogene in cerebellar Purkinje cells. Mol Cell Biol 9:4545–4549.

Takeya T, Hanafusa H (1983) Structure and sequence of the cellular gene homologous to the RSV *src* gene and the mechanism for generating the transforming virus. Cell 32:881–890.

Vardimon L, Fox LE, Moscona AA (1986) Accumulation of c-*src* mRNA is developmentally regulated in embryonic neural retina. Mol Cell Biol 6:4109–4111.

Veillette A, Bookman MA, Horak EM, Bolen JB (1988) The CD4 and CD8 T cell surface antigens are associated with the internal membrane tyrosine-protein kinase $p56^{lck}$. Cell 55:301–308.

Veillette A, Bookman MA, Horak EM, Samelson LE, Bolen JB (1989) Signal transduction through the CD4 receptor involves the activation of the internal membrane tyrosine-protein kinase $p56^{lck}$. Nature 338: 257–259.

Walaas SI, Lustig A, Greengard P, Brugge JS (1988) Widespread distribution of the c-*src* gene product in nerve cells and axon terminals in the adult rat brain. Mol Brain Res 3:215–222.

Wiestler OD, Walter G (1988) Developmental expression of two forms of $pp60^{c\text{-}src}$ in mouse brain. Mol Cell Biol 8:502–504.

Yang X, Walter G (1988) Specific kinase activity and phosphorylation state of $pp60^{c\text{-}src}$ from neuroblastomas and fibroblasts. Oncogene 3:237–244.